Kinetics of Cyanate and Imidazole Binding to Hemin in Micelles

Jon Simplicio,* Kathryn Schwenzer, and Francis Maenpa

Contribution from the Department of Chemistry, University of Miami, Coral Gables, Florida 33124. Received February 28, 1975

Abstract: Line broadening and chemical shifts are reported for cetyltrimethylammonium bromide, sodium dodecyl sulfate, and Triton X-100 micelles in the presence of ferro- and ferriprotoporphyrin IX. The specific micellar protons affected in the sodium dodecyl sulfate micelles suggest radial alignment of the metalloporphyrin along the hydrophobic tails interior to the micelle. Specific contact with the other micellar materials is less definitive. Association constants of dimeric hemin with the various micelles to produce an intercalated hemin–micelle complex have been measured using spectral techniques in the visible region and are consistent with a hemin to micelle ratio of 1:1. Visible spectral differences have been used to characterize and evaluate the association constants of cyanate and imidazole binding to the intercalated hemin being 1:1 and 2:1 complexes respectively of nucleophile to hemin. Formation and decomposition rate studies at 25° of the hemin–nucleophile complexes in micellar solutions have revealed pH dependent multistep processes with half-lives ranging from milliseconds to minutes which are extremely sensitive to the nature of the micelle. Cyanate binding and decomposition involving the iron center is particularly complex at physiological pH, suggesting the presence of linkage isomers.

Investigations of the chemical properties of most metalloporphyrins have often been limited to nonaqueous[1] solution due to limited solubility or dimerization.[2,3] In recent years a number of water soluble[3-5] derivatives such as the tetraphenyltetrasulfonated[5] porphyrin (TPPS) have been prepared to overcome the solubility limitation although dimerization still persists at high pH.[3] Several recent studies,[6-8] however, have shown that hemin, normally dimeric in basic aqueous solution and insoluble under acidic conditions, is solubilized over the entire pH range in monomer form in the presence of cationic CetMe₃NBr,[9] anionic SDS, and neutral Triton X-100 micelles. The iron center is susceptible to attack by a variety of nucleophiles and exhibits reversible binding with cyanide.[8] Recent investigations of model hemes with histidine residues axially bound to the iron have exhibited reversible oxygen carrying ability.[10,11] The imidazole moiety of histidine is also recognized as a major influence on enzymatic reactivity[12] The interaction between the imidazole residue and iron phthalocyanine[13-16,34] has been looked at in DMSO to more closely examine the nature of this interaction. We have undertaken a study of the intercalated hemin monomer with imidazole in aqueous solution over a wide pH region in an attempt to shed further light on imidazole-porphyrin interactions in hemoproteins. Cyanate binding studies at physiological pH have also been conducted to see what alternative role, if any it may have in its use for treatment of sickle cell anemia, other than carbamylation.

Results

Hemin Dimer–Monomer–Micelle Equilibrium. At 25°, 0.1 *M* TMAB, and pH 9 a series of isosbestic spectra was obtained as either SDS, CetMe₃NBr, or TX was added to a solution containing a fixed amount of hemin initially in the dimeric form No spectral changes in the dimer spectra are observed until the critical micelle concentrations are reached. Spectra were taken from 330 to 450 nm and plots of absorbance, at 400 nm, as a function of detergent are shown in Figure 1. The limiting spectra are taken to represent the molar extinction coefficient spectra of monodispersed ferriprotoporphyrin. The spectra for these end products are reported elsewhere.[6,8] The equilibrium consistent with the data is described by the following:[39]

$$Fe_{DIMER} + micelle'_f \rightleftharpoons 2H_2OMOH \cdot micelle \quad (1)$$
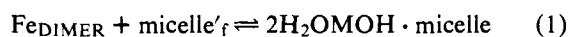
$$K_{eq} = \frac{[H_2OMOH \cdot micelle]^2}{[Fe_{DIMER}][micelle'_f]} \quad (2)$$

$$micelle'_{total} = (C_D - cmc)/N \quad (3a)$$

$$micelle'_f = micelle'_{total} - \frac{1}{2}(H_2OMOH \cdot micelle) \quad (3b)$$

C_d is the molar concentration of the detergent, micelle'$_f$ is the free micelle concentration, and cmc is the critical micellar concentration. N is the aggregation number of the micelle in 0.1 *M* TMAB at 25°, being 131,[17] 61,[18] and 139[36] for SDS, CetMe₃NBr, and TX, respectively, with the equilibrium constants for eq 2 being respectively 0.55 ± 0.1, 0.13 ± 0.02, 0.93 ± 0.30. These equilibrium constants are pH independent from about 8 to 11.5.

Some representative data are shown in Table I. The data suggest that the micelle bound with a hemin monomer intercalated has an aggregation number of about $\frac{1}{2}N$, due to the first order dependence on micelle $_f$ and the second order dependence on the monomer. Spectral and kinetic studies were all run at 2% SDS, 4% CetMe₃NBr, and 3% TX to ensure the presence of at least 95% intercalated monomer.

NMR of Hemin–Micelle Systems. Five per cent solutions of the three micelle systems, in D₂O at 34°, have the NMR assignments shown in Table II. These solutions were run in the absence of TMAB and under basic conditions of about 9-12 exhibiting no influence by pH in this region. Upon the addition of the ferriprotoporphyrin IX line broadening and chemical shifts occur as shown in Figures 2, 3, and 4. Hemin concentrations that approach and begin to exceed the calculated micellar concentration show appreciable changes in all protons. Excess sodium dithionite added to detergent solutions exhibits no effect on the micellar protons. Standard aliquots of hemin dimer solution were added to these solutions. Hemin is rapidly reduced in the closed NMR tubes. The behavior of the ferro form in affecting line broadening and chemical shifts is noticeably different than the oxidized form. NMR spectra at high metalloporphyrin concentration are shown in Figure 2 along with the 5% detergent solutions for comparison.

Equilibrium Data. The addition of either imidazole or potassium cyanate to hemin-detergent solutions, at constant pH, produced either red or orange colored solutions, respectively, with isosbestic curves shown in Figure 5 for cyanate. Limiting spectra are shown in Figures 6 and 7. Consistent with the spectral changes is the following:
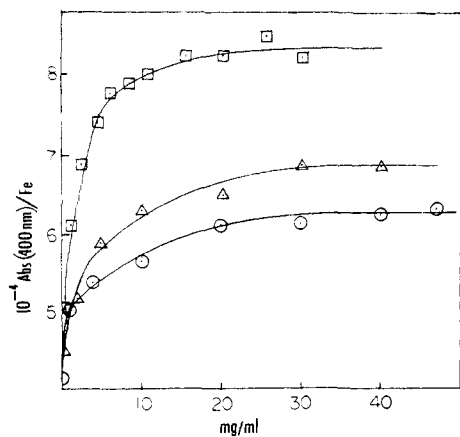
Figure 1. Spectral changes accompanying the addition of CetMe₃NBr (△), TX (○), and SDS (□) to solutions of constant hemin concentration at pH 9.50, 25°C.

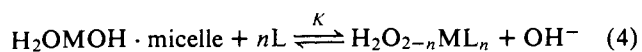Table I. Hemin Dimer—Monomer Equilibrium in SDS[a]

10^5 micelle$_f$ (M)	10^5Fe$_{dimer}$ (M)	10^5 H₂OMOH·micelle (M)	K_{eq}
1.13	0.277	0.446	0.64
3.63	0.196	0.608	0.52
8.86	0.118	0.764	0.56
14.10	0.0978	0.804	0.47
			0.55 Av

[a] Absorbance data taken at 400 nm, pH 10.50, 0.1 M TMAB, total porphyrin at 1.0 × 10⁻⁵ M.

Table II. NMR Assignments

CetMe₃NBr	CH₃(CH₂)₁₄CH₂N(CH₃)₃⁺Br⁻	(Hz)
	N(CH₃)₃	185.5
	(CH₂)₁₄	74
	CH₃	49
TX	(CH₃)CCH₂C(CH₃)₂—⟨⟩—O(CH₂CH₂O)ₙ—H	(Hz)
	(CH₃)₃C–	35
	(CH₃)₂C–	69.5
	(CH₂CH₂O)₁₀	210
SDS	CH₃(CH₂)₁₀CH₂SO₄⁻Na⁺	(Hz)
	CH₃	48
	(CH₂)₁₀	72
	CH₂	234.5

$$H_2OMOH \cdot micelle + nL \overset{K}{\rightleftharpoons} H_2O_{2-n}ML_n + OH^- \quad (4)$$

where $n = 1$ for L = cyanate, $n = 2$ for L = imidazole. With L = cyanate the final product may either be HOM(NCOH) or H₂OM(NCO). The possibility of N or O bound linkage isomers in both cases must also be considered. The concentrations of the free and bound hemin are readily calculated.[6,8] Representative data are shown in Table III. The equilibrium constants for imidazole are 8.86 M^{-1}, 4.85 × 10⁻² M^{-1}, and 0.44 M^{-1} for SDS, CetMe₃NBr, and TX, respectively. For cyanate, in the presence of CetMe₃NBr, the value is 1.67 × 10⁻⁴.

Kinetics of Formation of M(imid)₂·micelle. Reactions with imidazole in the presence of SDS or CetMe₃NBr were followed at wavelengths of either maximum product absorption or maximum reactant absorption. Both yield identical half-lives. Upon mixing on the stopped-flow device a rapid change in initial absorbance was observed to be complete within mixing time of about 5 msec. This reaction is ascribed to
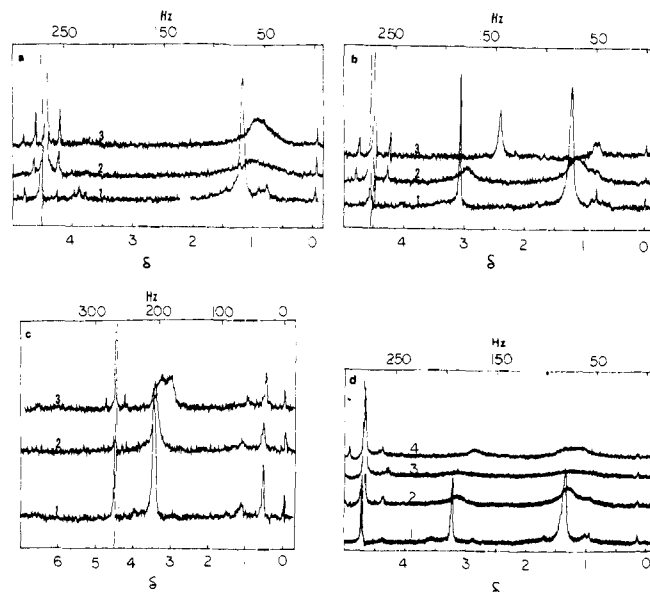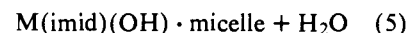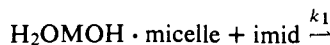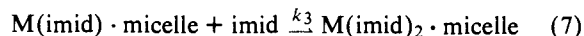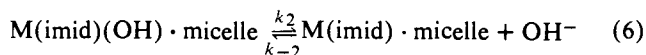

Figure 2. (a) NMR spectra of 5% SDS (1), 4.5 mM H₂OMOH·SDS (2), 4.5 mM reduced heme (3). (b) NMR spectra of 5% CetMe₃NBr (1), 4.5 mM H₂OMOH·CetMe₃NBr (2), 4.5 mM reduced heme (3). (c) NMR spectra of 5% TX (1), 2.2 mM H₂OMOH·TX (2), 2.2 mM reduced heme (3). (d) NMR spectra of 5% CetMe₃NBr (1), 1.45 mM H₂OMOH·CetMe₃NBr (2), 1.45 mM H₂OM(OCN)·CetMe₃NBr (3), 1.45 mM reduced heme–cyanate (4): pD 8.0, 0.1 M OCN⁻.

$$H_2OMOH \cdot micelle + imid \overset{k_1}{\rightarrow}$$

$$M(imid)(OH) \cdot micelle + H_2O \quad (5)$$

The subsequent reaction was fitted to the following two-step process,

$$M(imid)(OH) \cdot micelle \underset{k_{-2}}{\overset{k_2}{\rightleftharpoons}} M(imid) \cdot micelle + OH^- \quad (6)$$

$$M(imid) \cdot micelle + imid \overset{k_3}{\rightarrow} M(imid)_2 \cdot micelle \quad (7)$$

With a steady state on M(imid)·micelle the observed rate law (with excess imidazole) becomes,

$$\frac{1}{k_{obsd}} = \frac{k_{-2}[OH^-]}{k_2 k_3} \frac{1}{[imid]} + \frac{1}{k_2} \quad (8)$$

A plot of $1/k_{obsd}$ against $1/[imid]$, at constant pH, yields a straight line with intercept $1/k_2$ and a slope of $k_{-2}(OH^-)/k_2 k_3$. Figures 8 and 9 are the plots for SDS and CetMe₃NBr. The slopes, corrected for pH, are shown in Table IV along with the intercept values.

Base Decomposition of M(imid)₂·micelle. As eq 4 indicates the position of equilibrium may be shifted to the reactant side by the addition of base. Solutions containing either 100% of the bisimidazole complex or equilibrium mixtures were decomposed on the stopped-flow devices. Sodium hydroxide solutions either contained the same concentrations of detergent as the hemin–imidazole solutions or the hemin–imidazole solution had twice as much detergent as used in the formation and was mixed with sodium hydroxide containing no detergent. The data are presented in Table V. In all cases unimolecular processes were observed. For the M(imid)₂·SDS decomposition it was noted that under conditions where initially there is essentially 100% of the bis form the absorbance changes, as observed on the stopped-flow, in going from the bis to the product are not consistently in the right direction based on their spectral differences as measured on the Cary 17. The absorbance change at 530 nm is consistent with the spectral differences between the
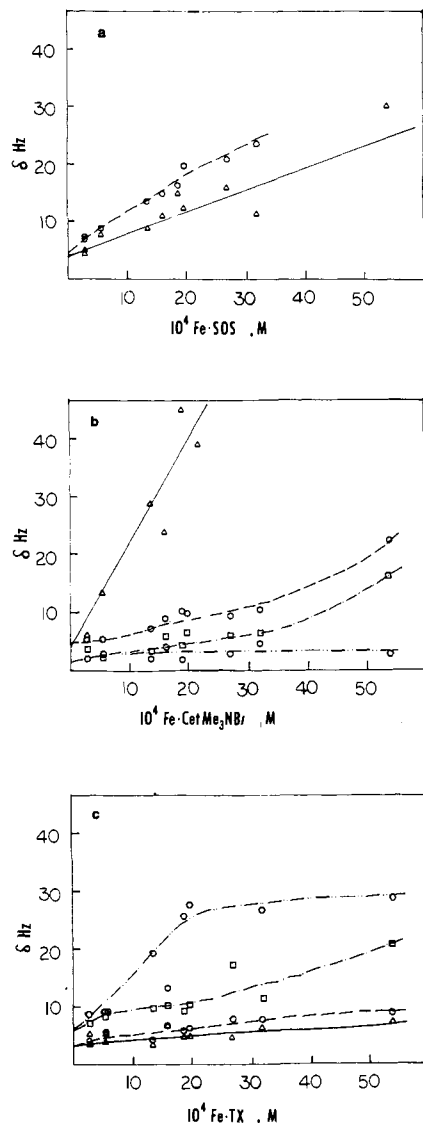
Figure 3. (a) Line broadening for SDS protons: by Fe(II) for $(CH_2)_{10}$ (Δ); by Fe(III) for $(CH_2)_{10}$ (O). (b) Line broadening for CetMe$_3$NBr protons: by Fe(III) for $N(CH_3)_3$ ($\square$); by Fe(II) for $N(CH_3)$ (O); by Fe(III) for $(CH_2)_{14}$ (O); by Fe(II) for $(CH_2)_{14}$ (Δ). (c) Line broadening for TX protons: by Fe(III) for $(CH_2CH_2O)_{10}$ ($\square$); by Fe(II) for $(CH_2CH_2O)_{10}$ (O); by Fe(III) for $CH_3)_3C$ (O); by Fe(II) for $(CH_3)_3C$ (Δ).

Figure 4. (a) Chemical shift for SDS protons: by Fe(II) for $(CH_2)_{10}$ (Δ); by Fe(III) for $(CH_2)_{10}$ (O). (b) Chemical shift for CetMe$_3$NBr protons: by Fe(III) for $N(CH_3)_3$ ($\square$); Fe(II) for $N(CH_3)_3$ (O); by Fe(III) for $(CH_2)_{14}$ (O); by Fe(II) for $(CH_2)_{14}$ (Δ). (c) Chemical shift for TX protons: by Fe(II) for $CH_2CH_2O)_{10}$ (O); by Fe(II) for $(CH_3)_3C$ (Δ).

reactants and products, however, that at 600 nm is not. However, when equilibrium solutions (ones comparable in $M(imid)_2$-micelle and $M(OH)(H_2O)$-micelle) are decomposed by base, the reverse occurs where now the 600 nm absorbance change is consistent with spectral differences while that at 530 nm is not. The rates of decomposition remain the same regardless of absorbance direction changes or initial concentrations of the bisimidazole complex to $M(OH)(H_2O)$-micelle.

Kinetics of Cyanate Binding to Hemin Intercalated in CetMe₃NBr. Kinetics of formation of the cyanate complex were investigated between pH 4 and 8. The bimolecular reaction observed for the binding appeared to be preceded by a unimolecular process of very small amplitude. This unimolecular process has a $t_{1/2} \simeq 10$ msec and is independent of hemin concentration, pH, or cyanate. A reaction of the same half-life was observed with hemin in 4% CetMe₃NBr mixed rapidly with CetMe₃NBr at 4% both under basic conditions. It could be observed with dimeric hemin mixed with an 8% CetMe₃NBr solution. The reaction appears to
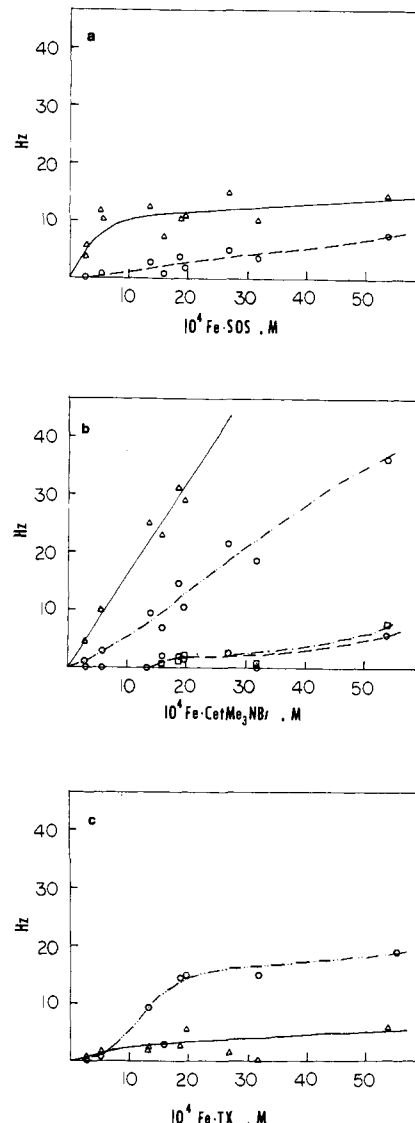
be a dilution perturbation of the dimer-monomer-micellar equilibrium and is not related to the actual cyanate binding.

The reactions, driven to completion, were followed at either 540 nm (the peak of the reactant) or 600 nm (the peak of the product) both yielding the same result. A mechanism consistent with the data is shown in Scheme I. Applying a steady state to the five-coordinate intermediates H_2O-M·micelle and HO-M·micelle one obtains eq 9.

$$k_{obsd} = \left[\frac{k_{2a}k_a[H^+][NCO^-]}{k_{-a} + k_{2a}[NCO^-]} + \frac{k_{2b}k_bK_a[NCO^-]}{k_{-b} + k_{2b}[NCO^-]}\right]\left[\frac{1}{[H^+] + K_a}\right] \quad (9)$$

K_a for the above reaction was determined previously[8] to be $7.95 \times 10^{-7} M^{-1}$. At high cyanate concentrations the reaction becomes cyanate independent with $k_{2a}(NCO^-) > k_{-a}$ and $k_{2b}(NCO^-) > k_{-b}$. Equation 9 reduces to,

$$([H^+] + K_a)k_{obsd}{}^{lim} = k_a(H^+) + k_bK_a \quad (10)$$

A plot of $([H^+] + K_a)k_{obsd}{}^{lim}$ (see Table VI) against $[H^+]$
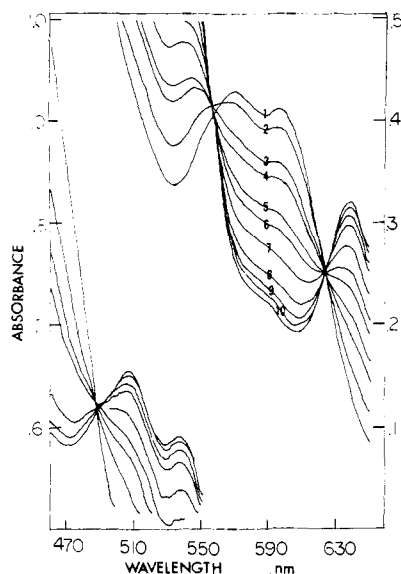
Figure 5. Family of curves showing isosbestic points in the equilibrium between $H_2OM(OCN)\cdot CetMe_3NBr$ and $H_2OMOH\cdot CetMe_3NBr$. For conditions see Table III.
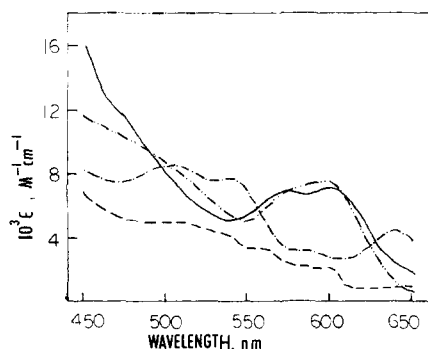
Figure 6. Spectra of $H_2OMOH\cdot CetMe_3NBr$ (—), $H_2OM(OCN)\cdot CetMe_3NBr$ (- · -) $H_2OM(OCN)'\cdot CetMe_3NBr$ (- · · -), and hemin-cyanate (- - -); pH 8.0.

Scheme I

$$M(OH)_2\cdot \text{micelle} \xrightleftharpoons{K_a} H_2OMOH\cdot \text{micelle} + H^+$$

$(+H_2)k_a \Big| k_n(-H_2O) \qquad (+H_2O)k_{-b} \Big| k_b(-H_2O)$

$H_2OM\cdot \text{micelle} \qquad\qquad HOM\cdot \text{micelle}$

$k_{2a} \Big| NCO^- \qquad\qquad k_{2b} \Big| NCO^-$

$$\text{product(s)}$$
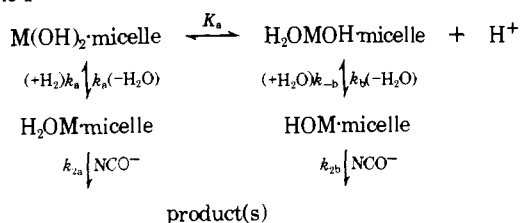
yields a straight line with slope $k_a \approx 5.8 \text{ sec}^{-1}$. At low cyanate concentrations the formation reaction is first order in cyanate as shown in Figure 10. (This figure does not include the $[H^+] + K_a$ factor of eq 9 for the convenience of putting all the data on the same plot. Table VI is calculated from slopes and limiting rates displayed in Figure 10 but includes the $[H^+] + K_a$ correction factor.) Under these conditions eq 10 reduces to

$$[[H^+] + K_a]k_{obsd} \approx \left[\frac{k_a k_{2a}[H^+]}{k_{-a}} + \frac{K_a k_b k_{2b}}{k_{-b}} \right] [NCO^-] \tag{11}$$

consistent with $k_{-a} > k_{2a}(NCO^-)$ and $k_{-b} > k_{2b}(NCO^-)$.

$k_{obsd}([H^+] + K_a)/[H^+]$ is relatively constant from pH 8 to 4 and all of the lines in Figure 10 essentially intercept the origin, within experimental error. This situation could only
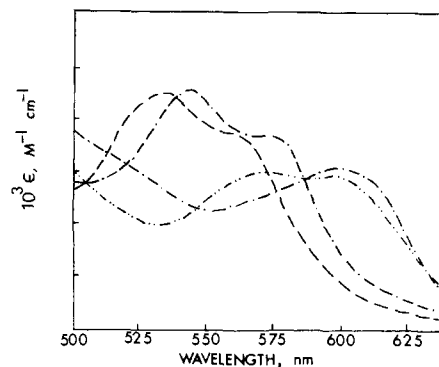

Figure 7. Limiting molar extinction spectra of $H_2OMOH\cdot SDS$ (- · -), $M(imid)_2\cdot SDS$ (- - -). $H_2OMOH\cdot CetMe_3NBr$ (- · · -), and $M(imid)_2\cdot CetMe_3NBr$ (- - · - -) at pH 9, 0.1 M TMAB.
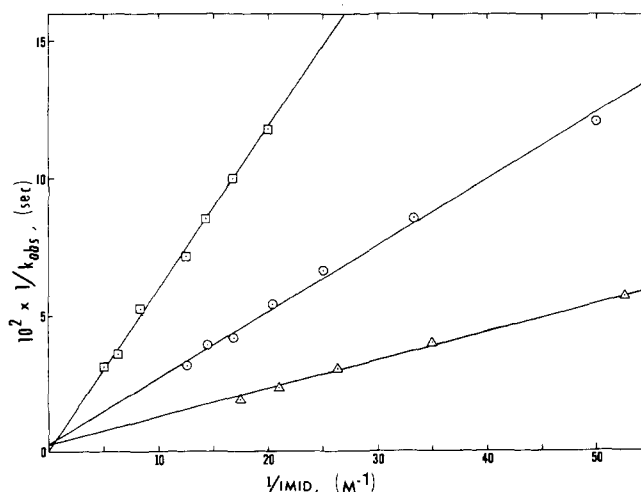

Figure 8. Plot of rate data for the formation of $M(imid)_2\cdot SDS$ from eq 8 at 25°: pH 8.5 for △, 9.0 for ○, and 9.5 for □.

hold if the second term in brackets in eq 11 is much smaller than the first term. Thus $(\Delta k_{obsd}/\Delta(NCO^-))(H^+ + K_a)/(H^+) \approx k_a k_{2a}/k_{-a}$. Factoring out k_a from $1.80 \times 10^2 \text{ sec}^{-1}$ (see Table VI footnote) yields $k_{2a}/k_{-a} \approx 30.9$.

Decomposition of $M(H_2O)(NCO)\cdot$micelle in $CetMe_3NBr$. Equation 4 indicates the cyanate product can be decomposed by the addition of base. The breakdown is characterized by a fast unimolecular process with $t_{1/2}$ about 10 msec and is independent of base from 10^{-5} to 0.5 M. As the base concentration used decreases so does the spectral amplitude. This reaction is followed by a slower unimolecular process which ultimately becomes base dependent as observed at either 540 or 600 nm. The data are plotted in Figure 11.

Temperature Jump Relaxation of $M(H_2O)(NCO)\cdot CetMe_3NBr$. A solution of the completely formed cyanate product was temperature jumped from 18 to 25°. A relaxation effect, $\tau = 10.2$ msec, was observed at two wavelengths, an increase in absorbance at 600 nm and a decrease at 540 nm. The relaxation time is independent of cyanate from 0.05 to 0.15 M and pH from 8.0 to 10.0. Below pH 8 the relaxation effect was not observed. A temperature jump was applied to a 4% CTAB, 0.1 M TMAB, and hemin solution with no observable effect.

Discussion

The hemin monomer-dimer equilibrium in the presence of micelles suggests that one hemin occupies a micelle with a new average aggregation number of about one-half of the

Table III. Equilibrium Parameters at 25° and 0.1 M TMAB

For Hemin and Cyanate in CetMe$_3$NBr

10^5 M(NCO) (M)	10^5 H$_2$OM(OH)	10^2 OCN$^-$free (M)	pOH	$10^4 K_{eq}$	Curve[a]
1.40	3.10	9.15	4.42	1.86	
1.90	2.60		4.67	1.75	
2.51	1.99		4.85	1.93	
3.12	1.38		5.04	2.43	
0.66	2.04	8.94	4.47	0.775	
1.10	1.60		4.74	1.02	
1.50	1.20		4.95	1.10	
7.15	1.85	12	4.10	1.69	1
6.40	2.60		4.29	1.72	2
5.25	3.75		4.62	1.42	3
4.84	4.16		4.69	1.45	4
3.55	5.45		4.9	1.60	5
2.22	6.78		4.99	2.59	6
2.15	6.85		5.25	1.48	7
1.24	7.76		5.41	2.02	8
0.90	8.10		5.60	1.87	9
4.10	5.60	1.0	6.00	1.0	
6.90	2.80	2.0	6.00	1.23	
8.35	1.35	4.0	6.00	1.54	

$K_{av} = 1.67 \times 10^{-4}$

For Hemin and Imidazole in SDS

10^5 M(imid)$_2$ (M)	10^5H$_2$OMOH (M)	10^3 imidfree (M)	pOH	K, M^{-1}
0.98	9.39	0.980	3.98	11.39
2.90	7.47	0.942	4.72	8.33
4.22	6.15	0.916	4.96	8.98
5.45	4.92	0.891	5.19	9.01
6.64	3.73	0.867	5.52	7.15
1.18	9.19	2.98	3.20	9.15
3.68	6.69	2.93	3.79	10.42
5.56	4.81	2.89	4.12	10.51
7.45	2.92	2.85	4.52	9.48
8.53	1.84	2.83	4.89	7.46
1.74	8.63	4.96	2.96	8.96
3.60	6.77	4.93	3.39	8.92
5.20	5.17	4.89	3.68	8.77
6.65	3.72	4.87	3.93	8.87
8.31	2.06	4.83	4.32	8.26
2.85	12.7	0.443	5.00	11.40
3.94	11.6	0.421	5.30	9.59
4.95	10.6	0.401	5.55	8.18
4.12	11.4	3.94	3.41	9.10
4.61	10.9	3.93	3.47	9.35
6.90	8.65	3.89	3.81	8.28
7.68	7.87	3.88	3.88	8.69
11.9	3.66	3.76	4.53	6.78
5.92	14.8	9.88	2.60	10.30
10.5	10.2	9.79	3.11	8.34
12.9	7.75	9.74	3.37	7.51
16.2	4.50	9.68	3.69	7.85
17.9	2.75	9.64	4.00	7.06

$K_{av} = 8.86 \ M^{-1}$

[a] See Figure 5.

Figure 9. Plot of rate data for the formation of M(imid)$_2$·CetMe$_3$NBr from eq 8 at 25°: pH 8.0 for O, 8.5 for △, and 9.0 for □.

Table IV. Summary of Formation Data of Imidazole Binding

Micelle	pH	
		$10^{-2}k_{-2}/k_2k_3$,[a] sec
SDS	9.50	1.82
	9.00	2.40
	8.50	2.90
		$10^{-5}k_{-2}/k_2k_3$, sec
CetMe$_3$NBr	9.0	2.4
	8.5	5.3
	8.0	4.5
	$k_2 = 0.25 \pm 0.08$ sec^{-1} [b]	

[a] Values are known to ±10%. [b] Obtained by least-squares analysis.

Table V. Acid and Base Decomposition of M(imid)$_2$·micelle

Micelle	10^6[OH$^-$],[a] M	Fast k_{obsd}, sec^{-1}	Slow $10^2 k_{obsd}$, sec^{-1}
CetMe$_3$NBr	2.8	33	—
	79.5	41	1.24
	100	36	1.87
	560	46	1.54
	[HCl],[b] M		
	0.05	31.8	
	0.10	34.8	
	0.20	32.7	
	0.30	35.0	
	0.50	38.1	
	10^2[OH$^-$],[a] M	k_{obsd}, sec^{-1}	k_{obsd}, sec^{-1}
SDS	0.50	3.9c	3.3d,e
	1.0	3.9	3.4e
	1.5	3.8	3.5e
	2.0	3.8	3.1e
	2.5		3.3
	3.0		3.2
	4.0		3.0

[a] Followed at 530 and 600 nm. [b] Followed at 400, 490, 570, and 640 nm. [c] 2% SDS in both base and hemin–imidazole solutions. [d] 4% SDS in hemin–imidazole solution and 0% in base. [e] 4% SDS in hemin–imidazole solution and 4% in base give same result.

original value. This is indicated by the first-order dependence on the calculated micelle concentration and the second-order dependence on the monomer form in eq 2. Micelle sizes and structures are known[21] to be sensitive to the nature and charge of the added electrolytes. The molecular weight of SDS can vary between 14200 and 25500[22] in the presence of 9.66 × 10^{-4} M Zn^{2+} to 38000 in 0.1 M NaCl.[17] Solubilization studies[23] of benzene in a variety of micelles indicate that the solubilizate does affect the size of the micelle and that the benzene to micelle ratio varies between 2.1 and 2.7. It is reasonable to expect the micelle to contain at most a single hemin considering its size relative to benzene. A hemin dimer–monomer equilibrium in a water–ethanol mixture (48.8 mol % alcohol) giving
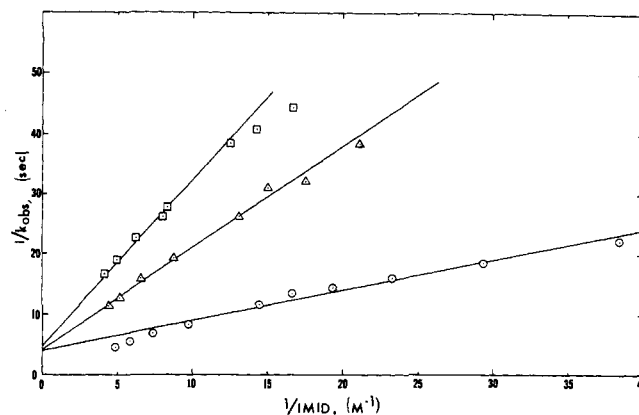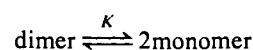
$$\text{dimer} \underset{}{\overset{K}{\rightleftharpoons}} 2\text{monomer}$$

($K = 0.04\ M$) gives a solution which is roughly 10% in the dimer form.[14] A 1.4 × 10^{-4} M micellar solution of SDS will produce the same percentage dimer–monomer concentrations. The hydrophobic micellar environment apparently solvates hemin more than the polar water–ethanol mixture. Since both the size of the micelle (i.e., one that contains the hemin) and the charge on the Stern layer are both likely to
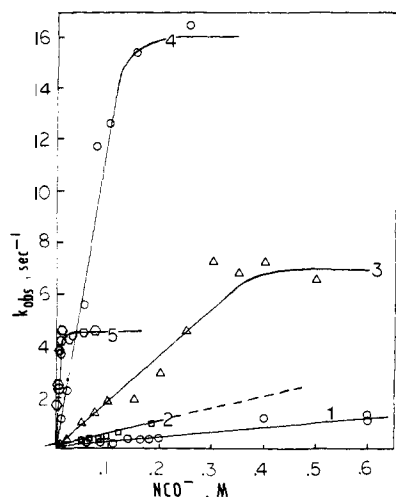
Figure 10. Plot for eq 10 from stopped-flow data at 25°C, 0.1 M TMAB, and 4% CetMe₃NBr: curve 1 at pH 8.0; curve 2 at pH 7.5; curve 3 at pH 7.0; curve 4 at pH 6.0; curve 5 at pH 5.0. For convenience of display purposes $[H^+] + K_a$ is not included in the plot. Table VI summarizes slopes and limiting rates taking $[H^+]$ and K_a into account.

Table VI.

pH	$10^{-6}[\Delta k_{obsd}/ \Delta(NCO^-)] [H^+ + K_a]$ sec^{-1}	$10^{-2}[\Delta k_{obsd}/ \Delta(NCO^-)] [H^+ + K_a]/ [H^+]$ M^{-1} sec^{-1}	$[H^+ + K_a](k_{obsd}^{lim})$ M sec^{-1}
8.0	1.86	1.86a	—
7.5	4.48	1.41	—
7.0	16.8	1.68	6.27×10^{-6}
6.0	225	2.25	2.87×10^{-5}
5.0	3920	3.92b	4.86×10^{-5}
4.0	~48700	4.87b	1.21×10^{-3}

a The average value from pH 8 to 6 is $1.80 \times 10^2 M^{-1}$ sec^{-1}.
b Scatter in the data makes these numbers somewhat unreliable. Also evidence presented later on suggests the appearance of new mixed protonated hemin–cyanate–micelles that could contribute to altering these slopes under highly acidic conditions.

affect the monomer–dimer equilibrium it is difficult to unambiguously rationalize the order of the equilibrium constants, TX > SDS > CetMe₃NBr at 25°.

The observation that the methylene hydrogens of SDS are affected indicates that the porphyrin is not associated with the anionic Stern layer. The NMR data tend to show little or no effect on either the internal methyl group or on the methylene protons adjacent to the sulfate group up to high concentrations of metalloporphyrin. Since the paramagnetic influence falls off as $1/r^6$ this tends to support a radial type alignment of the hemin in the micellar aggregate rather than immersed in the center of the core.[33] Such an arrangement has been suggested for benzoic acid[24] in SDS with the carboxylic acid end in the Stern layer and the benzene ring dissolved in the hydrophobic core.

Up to appreciable concentrations of either heme or hemin the N-methyl protons of CetMe₃NBr are not affected. However, at about 0.02 M hemin these protons, as well as the methylene protons of the aliphatic chain, begin to undergo substantial broadening. This suggests micellar disruption and/or hemin aggregation at the micelle surface. Heme has little effect on the line broadening of the N-methyl protons at concentrations up to 0.05 M but has substantial effect on the chemical shift on these same protons almost immediately upon the addition of minute quantities of heme. In TX the protons in the ethoxy chain are broad-
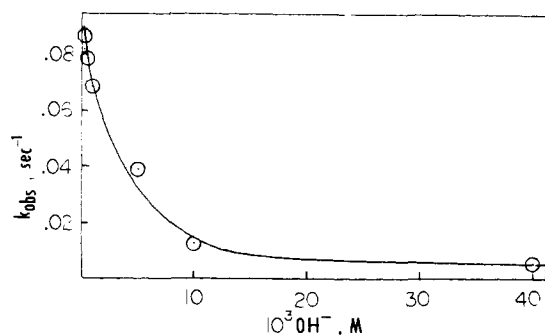

Figure 11. Base decomposition of hemin-cyanate complex in 4% CetMe₃NBr and 0.1 M TMAB.

ened compared to the branched alkane end presumably because of the proximity of the porphyrin. It is known that the ethoxy end is in extensive contact with solvent.[32] These protons are even more dramatically affected by heme. The NMR data provide evidence to confirm a close association between the hemin and the micelle as suggested by the visible spectral data presented here.
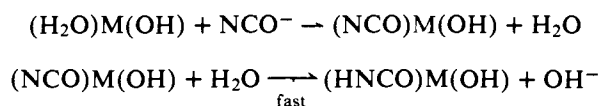
While each of the detergent micelles of SDS, CetMe₃NBr, and TX readily solvate and monomerize the dimer, there appears to be no obvious correlation of the equilibrium constant to either charge on the Stern layer or aggregation number. No doubt these all play an important role. A recent study[37] with the water soluble sodium tetra(p-sulfophenyl)porphyriniron(III) has found that this dimer system is not monomerized under basic conditions by the addition of similar detergents. Another added parameter needed to understand the solvation properties of the micelles with respect to porphyrins is the substituent effect on the porphyrins. The micelles associated with the comparably large hemin no doubt have a considerably different arrangement from their usual spherical or elipsoidal geometry. It is likely that this disruption introduces significant quantities of solvent into the proximity of the hemin–micelle complex. Hemin appears to be completely insoluble in benzene[38] but when methanol is added it readily dissolves due to its solubility in a methanol pool that is surrounded by the surfactant molecules. Two imidazole ligands bind in the final product as was found with cyanide.[8] However, only one cyanate is bound to the hemin in the micellar solution of CetMe₃NBr. In contrast to the study of only one imidazole binding to a water soluble porphyrin[4] our results coincide with the stoichiometry found in nonaqueous solvents,[13] water–ethanol mixed solvents,[14] and X-ray data[25] for a wide variety of iron porphyrins. The instability of a mono-imidazole complex is believed to be a result of a high spin to low spin conversion resulting from the first imidazole binding and favoring a second one to bind immediately.[13] That only one cyanate binds is consistent with the fact that cyanate imposes a weak ligand field incapable of changing the spin state and thus not favoring the binding of a second cyanate. Alternatively, if the structural arrangement of the monocyanate complex is HOM(NCOH) then it is reasonable not to expect an additional cyanate to displace the OH⁻ which is a much stronger coordinating ligand. If the bimolecular rate constant for the first imidazole binding to hemin in CetMe₃NBr is taken to be about 3×10^4 M^{-1} sec^{-1},[15] then at the concentrations of imidazole used in the present study the half-life would be about 1 msec and is beyond the time resolution of the stopped-flow device. This is consistent with the large absorbance change observed to occur within mixing time in the formation study. The pH corrected slopes of Table IV should all be the same, but, while no trend is evident, the data indicate small differences

outside experimental error. This deviation may be a reflection of the pH differences at the micelle-water interface[19,26] due to the lowering of the effective dielectric constant at the surface. It may also be due to the variation of the pK_a of imidazole known to be sensitive to the micellar environment.[27]
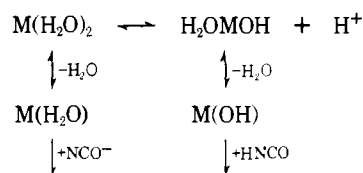
M(imid)$_2$·micelle is decomposed by the addition of base to shift equilibrium 4 to the left or by the addition of acid which acts to protonate free imidazole. The absorbance changes in going from product to reactant side are not consistent with the spectral differences between product and reactant as found on the Cary 17. The direction is dependent upon the initial ratio of hemin to the bisimidazole product although the rates remain the same regardless of the direction of the absorbance change. The spectral changes associated with base decomposition can be rationalized by invoking the existence of an unstable monoimidazole intermediate whose spectral properties[29] are different from either final reactant or product and whose concentration varies with the initial conditions. An observable monoimidazole transient intermediate is not unexpected in view of the stable product found with an ethylenediamine substituted protoporphyrin IX.[4] Table V shows a unimolecular decomposition which may be the first imidazole coming off of M(imid)$_2$·SDS. The apparent dissociation rate constant for the myoglobin[28] monoimidazole complex is 4.3 sec^{-1} at pH 8 compared to 3.9 sec^{-1} in the present study. This observed reaction may be the first imidazole dissociating although the spectral changes parallel those observed for the loss of the second imidazole in CetMe$_3$NBr. The decomposition of M(imid)$_2$·CetMe$_3$NBr exhibits a fast unimolecular process identical for both acid and base decomposition suggesting a common rate determining step, presumably the first imidazole coming off. This is followed by a slower unimolecular process with a rate constant 1.54×10^{-2} sec^{-1}, presumably being the second imidazole coming off. The second imidazole dissociation is not observed under acidic conditions and may reflect a translabilizing effect by water in the acid path as opposed to a hydroxy group in the base path. Assuming 1.54×10^{-2} sec^{-1} to represent k_{-1} (the reverse of eq 5) and the faster base decomposition rate of 38 sec^{-1} being k_{-3} with $k_{-2}/k_2k_3 = 5 \times 10^5$ sec and k_1 as assumed earlier 3×10^4 M^{-1} sec^{-1}, then the overall kinetically estimated equilibrium constant, i.e., $k_1k_2k_3/k_{-1}k_{-2}k_{-3}$, of eq 4 is calculated to be 10.2×10^{-2} M^{-1} compared to 4.85×10^{-2} M^{-1} determined spectrally.

The large difference in base decomposition of the bisimidazole complex between the SDS and CetMe$_3$NBr micelles is likely a reflection of the charge differences at the Stern layer of the micelles as well as the hydrophobicity differences imposed upon the hemin by the two types of micelles. The greater thermodynamic stability of the bis complex in SDS compared to CetMe$_3$NBr parallels the slower decomposition of the imidazole from M(imid)$_2$·SDS.
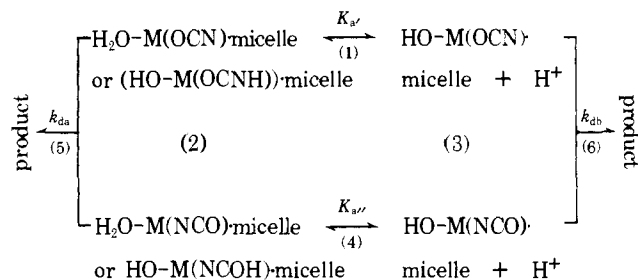
In the lower pH region around 5, where appreciable concentrations of HNCO are present, an inherent kinetic ambiguity exists via the acid path for the hemin–cyanate formation reaction (Scheme II). However, we prefer the scheme in which H$_2$OMOH reacts only with NCO$^-$ since in the equilibrium studies carried out at high pH, where no HNCO exists, the NCO$^-$ anion clearly binds to the hemin with the liberation of hydroxide. It is likely that the NCO$^-$ does not directly displace the much stronger nucleophile hydroxide but rather operates overall by:

$$(H_2O)M(OH) + NCO^- \rightarrow (NCO)M(OH) + H_2O$$

$$(NCO)M(OH) + H_2O \xrightarrow{\text{fast}} (HNCO)M(OH) + OH^-$$

Scheme II

$$M(H_2O)_2 \longrightarrow H_2OMOH + H^+$$

$$\downarrow{\scriptstyle -H_2O} \qquad\qquad \downarrow{\scriptstyle -H_2O}$$

$$M(H_2O) \qquad\qquad M(OH)$$

$$\downarrow{\scriptstyle +NCO^-} \qquad\qquad \downarrow{\scriptstyle +HNCO}$$

Scheme III

The decomposition of the cyanate complex by base is characterized by a unimolecular reaction with a 10-msec half-life followed by a slower first-order process, above a base concentration 0.02 M, of a 116 sec half-life. Using a continuous flow, the spectrum of a transient intermediate was taken within approximately 5 sec after its generation and is shown in Figure 6. Above pH 8, with cyanate concentrations that will produce 100% of the hemin–cyanate product, temperature-jump relaxation effects are observed and are independent of cyanate yielding $\tau^{-1} = 98$ sec^{-1}. The relaxation effect considered together with the fast unimolecular process that precedes base decomposition and the spectral evidence of a transient intermediate suggests a linkage isomerization process involving the N and O ends of the ambidentate cyanate. As the pH of a hemin–cyanate solution is lowered below 8 the relaxation effect is no longer observed despite the fact that the cyanate product is still present. A protonated form of the cyanate may be bound to the hemin favoring one isomer over the other and preventing isomerization. While there is no evidence in the literature concerning the existence of a protonated coordinated cyanate in aqueous solution, the hydrophobic environment may well favor such a species that would reduce the charge density in the micelle. The dissociation of cyanate from sperm whale metmyoglobin[30] increases as the pH decreases and has been interpreted to mean that the acid form of the coordinated ligand is more labile than the basic form. These observations are consistent and tend to support the presence of a protonated coordinated cyanate in the hydrophobic micellar environment.

Scheme III represents a possible dissociation route consistent with the general behavior of the base decomposition, spectra, relaxation behavior, and isomerization. The fast unimolecular process is suggested to be a combination of steps 2 and 3 which are induced by the two diffusion controlled acid–base reactions of steps 1 and 4. The shifting of equilibria of 1 and 4 upon the addition of base, prior to decomposition, is therefore what gives rise to the linkage isomerization of steps 2 and/or 3. $k_{obsd} = (k'[H^+] + k'')/([H^+] + k''')$ where the various k's are composites depending upon whether two or more species undergo decomposition at comparable rates. As H$^+$ diminishes one predicts k_{obsd} to become base independent and equal to k''/k''' (the value being 6×10^{-3} sec^{-1}). As H$^+$ gets larger k_{obsd} will increase and then level off. This leveling off is not observed

Simplicio, Schwenzer, Maenpa / Cyanate and Imidazole Binding to Hemin in Micelles

since at low pH protonated forms of the carboxylic acid substituents may be altering the hemin reactivity.

Carbamylation reactions, which are related to the inhibition of sickle cell anemia are relatively slow (5 min[31,35]), in comparison to cyanate binding to metmyoglobin and intercalated hemin. It is possible that carbamylation of hemoglobin S is preceded by rapid binding of cyanate to the metalloporphyrin. At present we are continuing to investigate the role that the micellar environment plays in modulating the reactivity of the metalloporphyrin by studying the reactivity of water soluble porphyrins in the presence and absence of micelles with a variety of nucleophiles.

Experimental Section

Materials. Sodium dodecylsulfate, Triton X-100, cetyltrimethylammonium bromide, tetramethylammonium bromide, and imidazole (free base) were obtained from Sigma Chemical Company and were used without further purification. The ferriprotoporphyrin IX was isolated from cows blood by the method of Labbe and Nishida.[20] Standardized solutions of hemin were carefully prepared as described previously.

Physical Measurements. pH measurements were obtained with a Radiometer pH Meter 26 using a GK 2301B glass combination electrode previously standardized with the appropriate Beckman prepared buffer. Visible and uv spectral properties of the various solutions were obtained with a Cary 17 recording spectrophotometer. Rates longer than about 2 min were measured by using the Cary 17. Rapid reactions were followed with either a stopped-flow or a temperature-jump device previously described.[7] Normally three sets of reactions were run to give the best average half-life or relaxation time. Temperatures for spectral and flow work were controlled at 25° to ±0.1°. Stopped-flow reactions were run under pseudo-first-order conditions in either cyanate or imidazole. The reactions were driven to completion (this information was calculated on the basis of equilibrium data from this work) to avoid the complications of reversible kinetics. All solutions used for spectral or kinetic measurements contained 0.1 M tetramethylammonium bromide.

NMR Data. NMR spectra were taken in D_2O at 34° with an Hitachi Perkin-Elmer 60 megacycle high resolution spectrometer. Concentric NMR tubes were used for all measurements with TMS in $CDCl_3$ in the external tube for reference. Internal use of TMS in the metalloporphyrin-detergent solutions appeared to yield slightly different chemical shift results. All work reported here is for TMS as an external reference.

References and Notes

(1) J. M. Duclos, *Bioinorg. Chem.*, **2**, 263 (1973).
(2) S. R. Brown, T. C. Dean, and P. Jones, *Biochem. J.*, **117**, 733 (1970).
(3) W. I. White and R. A. Plane, *Bioinorg. Chem.*, **4**, 21 (1974).
(4) G. B. Kolski and R. A. Plane, *J. Am. Chem. Soc.*, **94**, 3740 (1972).
(5) E. B. Fleischer, J. M. Palmer, T. S. Srivastava, and A. Chatterjee, *J. Am. Chem. Soc.*, **93**, 3162 (1971).
(6) J. Simplicio, *Biochemistry*, **11**, 2525 (1972).
(7) J. Simplicio, *Biochemistry*, **11**, 2529 (1972).
(8) J. Simplicio and K. Schwenzer, *Biochemistry*, **12**, 1923 (1973).
(9) The intercalated hemin monomer (with changes omitted) will be denoted H_2OMOH-micelle. The following abbreviations will be used: sodium dodecyl sulfate (SDS), cetyltrimethylammonium bromide (CetMe₃NBr), Triton X-100 (TX). Tetramethylammonium bromide TMAB, imidazole (imid), and the hemin dimer is designated Fe$_{DIMER}$.
(10) C. K. Chang and T. G. Traylor, *J. Am. Chem. Soc.*, **95**, 8475 (1973).
(11) Reference 10, p 8477.
(12) R. J. Sundberg and R. B. Martin, *Chem. Rev.*, **74**, 471 (1974).
(13) J. G. Jones and M. V. Twigg, *Inorg. Chem.*, **8**, 2120 (1969).
(14) B. B. Hasinoff, H. B. Dunford, and D. G. Horne, *Can. J. Chem.*, **47**, 3225 (1969).
(15) N. S. Angerman, B. B. Hasinoff, H. B. Dunford, and R. B. Jordan, *Can. J. Chem.*, **47**, 3217 (1969).
(16) R. J. Sundberg and R. B. Martin, *Chem. Rev.*, **74**, 486 (1974).
(17) H. Schott, *J. Phys. Chem.*, **70**, 2966 (1966).
(18) K. J. Mysels and L. H. Princen, *J. Phys. Chem.*, **63**, 1696 (1959).
(19) C. A. Bunton and B. Wolfe, *J. Am. Chem. Soc.*, **95**, 3742 (1973).
(20) R. E. Labbe and G. Nishida, *Biochem. Biophys. Acta*, **26**, 437 (1957).
(21) F. Reiss-Husson and V. Luzzati, *J. Phys. Chem.*, **68**, 3504 (1964).
(22) M. U. Oko and R. L. Venable, *J. Colloid Interface Sci.*, **35**, 53 (1971).
(23) R. L. Venable and R. V. Nauman, *J. Phys. Chem.*, **68**, 3498 (1964).
(24) A. S. Waggoner, O. H. Griffith, and C. R. Christensen, *Proc. Natl. Acad. Sci. U.S.A.*, **57**, 1198 (1967).
(25) R. M. Collins, R. Countryman, and J. L. Hoard, *J. Am. Chem. Soc.*, **94**, 2066 (1972).
(26) P. Mukerjee and K. Banerjee, *J. Phys. Chem.*, **68**, 3567 (1964).
(27) J. H. Fendler, F. Nome, and H. C. Van Woert, *J. Am. Chem. Soc.*, **96**, 6745 (1974).
(28) W. F. Diven, D. E. Goldsack, and R. A. Alberty, *J. Biol. Chem.*, **240**, 2437 (1965).
(29) C. E. Castro, *Bioinorg. Chem.*, **4**, 45 (1974).
(30) D. E. Goldsack, W. S. Eberlein, and R. A. Alberty, *J. Biol. Chem.*, **240**, 4312 (1965).
(31) C. K. Lee and J. M. Manning, *J. Biol. Chem.*, **248**, 5861 (1973).
(32) F. Podo, A. Ray, and G. Nemethy, *J. Am. Chem. Soc.*, **95**, 6164 (1973).
(33) M. B. Lowe and J. N. Phillips, *Nature (London)*, **30**, 444 (1934).
(34) G. N. La Mar and F. A. Walker, *J. Am. Chem. Soc.*, **94**, 8607 (1972).
(35) M. H. Garner, W. H. Garner, and F. R. N. Gurd, *J. Biol. Chem.*, **248**, 5451 (1973).
(36) L. M. Kushner and W. D. Hubbard, *J. Phys. Chem.*, **58**, 1163 (1954).
(37) P. Hambright, M. Krishnamurthy, and P. B. Chock, *J. Inorg. Nucl. Chem.*, **37**, 557 (1975).
(38) W. Hinze and J. H. Fendler, *J. Chem. Soc., Dalton Trans.*, 238 (1975).
(39) Minor decreases in the extinction coefficient of the hemin dimer spectrum are observed to occur upon the addition of micromolar concentrations of any detergent. This has been attributed to detergent association with the dimer with the hemin dimer integrity maintained. The drop in the extinction coefficient has been suggested to be a result of an increase in the iron–oxygen–iron distance of the bridge as water in the solvation shell is replaced stepwise by detergent molecules. As the dimer separates the electronic transitions become less allowed. At 400 nm spectra of the original dimer and that of the detergent solvated dimer exhibit an isosbestic point. Thus this wavelength may be used without concern in obtaining the equilibrium constant for the dimer–monomer equilibrium constant with micelles. We express our thanks to Dr. George Clarke for suggesting the reasons for the observed changes in the spectra of the original dimer.